Available online at www.sciencedirect.com
ScienceDirect
International Journal of Heat and Mass Transfer 50 (2007) 4256–4264
International Journal of HEAT and MASS TRANSFER
www.elsevier.com/locate/ijhmt

# Condensation heat transfer and pressure drop of R134a in annular helicoidal pipe at different orientations

C.X. Lin [a], M.A. Ebadian [b,*]

[a] Department of Mechanical, Aerospace, and Biomedical Engineering, University of Tennessee, Knoxville, TN 37996, United States
[b] Department of Mechanical and Materials Engineering, Florida International University, Miami, FL 33174, United States

Received 17 August 2006; received in revised form 16 February 2007
Available online 4 May 2007

**Abstract**

Experimental investigations were conducted to determine the condensation heat transfer and pressure drop of refrigerant R134a in annular helicoidal pipe at three inclination angles. The experiments were performed with the Reynolds number of R134a ranging from 60 to 200, and that of cooling water from 3600 to 22 000; temperatures of R134a at 30 °C and 35 °C, and cooling water at 16 °C, 20 °C and 24 °C. The experimental results indicated that the refrigerant Nusselt number was larger at lower refrigerant saturation temperature, and would increase with the increase of mass flow rates of refrigerant and cooling water. It was found that the refrigerant heat transfer coefficient of annular helicoidal pipe could be two times larger than that of equivalent plain straight pipe when the refrigerant Reynolds number was larger than 140. Comparison with identical helicoidal pipe with opposite flow channel arrangement revealed that the refrigerant heat transfer rate was larger when the refrigerant was flowing in the annular section at the cooling water Reynolds number larger than 4000, but the pressure drop was always larger in this flow channel arrangement.
Published by Elsevier Ltd.

*Keywords:* Annular helicoidal pipe; Helical pipe; Condensation; Two-phase flow

## 1. Introduction

Helicoidal pipes have been extensively studied and used in a variety of engineering areas, such as refrigeration, air conditioning, nuclear power generation, petrochemical, pharmaceutical and aerospace industries, due to their high efficiency in heat transfer and compactness in volume.

Uddin et al. [2] experimentally determined the variation of local condensation heat transfer coefficient of R134a in helically coiled tubes and reported that the local condensation heat transfer coefficient increased with the decrease of helical coil and tube diameters. Zaki et al. [3] conducted experimental investigations of condensation heat transfer of R134a flowing inside helicoidal pipes, and reported that the average condensation heat transfer coefficients could be enhanced compared with that inside straight smooth tubes. Kang et al. [4] experimentally studied the heat transfer and pressure drop characteristics of R134a in helicoidal pipes and provided heat transfer correlations from the experimental data. It was also reported that with the increase of cooling water Reynolds number, the refrigerant heat transfer coefficients decreased. Yu et al. [5] experimentally investigated the condensation heat transfer of R134a in a helicoidal pipe and reported that the orientation of helicoidal pipe has a significant effect on both refrigerant and overall heat transfer coefficients. Recently, Wongwises and Polsongkram [6] reported experimental study of condensation heat transfer and pressure drop of HFC-134a in a helically coiled heat exchanger with larger mass flow rate than Kang et al. [4].

Annular helicoidal pipes could not only provide more compactness in volume, but also controlled main flow and secondary flow due to the inner-wall boundary effects, making the friction factor and heat transfer characteristics different from straight circular tubes [7]. Garimella et al. [8]

* Corresponding author. Tel.: +1 305 348 3696; fax: +1 305 348 1932.
*E-mail address:* ebadian@fiu.edu (M.A. Ebadian).

0017-9310/$ - see front matter Published by Elsevier Ltd.
doi:10.1016/j.ijheatmasstransfer.2007.02.022

**Nomenclature**

| | |
|---|---|
| $A$ | heat transfer area, $m^2$ |
| $B$ | pitch of helicoidal pipe, m |
| $C_p$ | specific heat, J/(kg °C) |
| $d$ | tube diameter, m |
| $D$ | coil diameter, m |
| $f_t$ | friction factor |
| $G$ | refrigerant mass flux, kg/($m^2$ s) |
| $h_{fg}$ | latent heat, kJ/kg |
| $H$ | heat transfer coefficient, W/($m^2$ °C) |
| $K$ | thermal conductivity, W/(m °C) |
| $Nu$ | Nusselt number |
| $P$ | pressure, Pa |
| $Pr$ | Prandtl number |
| $Q$ | heat transfer rate, W |
| $R$ | heat transfer resistance of tube wall, $m^2$ °C/W |
| $Re$ | Reynolds number |
| $T$ | temperature, °C |
| $U_0$ | overall heat transfer coefficient, W/($m^2$ °C) |
| $\dot{V}$ | volumetric flow rate, $m^3$/s |
| $z$ | coordinate in $z$-direction, m |

*Greek symbols*

| | |
|---|---|
| $\rho$ | density, kg/$m^3$ |
| $\beta$ | inclination angle of the test section |
| $\phi$ | pressure drop multiplier, $\sqrt{(\frac{dp}{dz})_f/(\frac{dp}{dz})_{L(G)}}$ |
| $\chi$ | Lockhart–Martinelli parameter, $\sqrt{(\frac{dp}{dz})_L/(\frac{dp}{dz})_G}$ |

*Subscripts*

| | |
|---|---|
| 1 | internal tube; condition 1 |
| 2 | external tube; condition 2 |
| crit | critical |
| f | refrigerant |
| in | inner tube |
| out | outer tube |
| s | saturation |
| w | water |
| wall | wall condition |
| D | pressure drop |
| G | vapor phase |
| L | liquid phase; laminar flow |
| T | turbulent flow |
| Tr | transitional flow |

investigated the forced convection heat transfer in coiled annular ducts for laminar and transition flows, and reported that coiling augments the heat transfer coefficients above the values for a straight annulus especially in the laminar region. Choi et al. [9] numerically studied the steady laminar flows in coiled annular ducts and observed the evolution of secondary flow and the effect of radius ratio on the flow development. It was concluded that the flow in a curved annular duct is not necessarily fully developed earlier when the radius ratio was larger owing to the complicated interaction between the viscous and centrifugal forces. For annular helicoidal pipe, the experimental results of Xin et al. [10] indicated that the single-phase and two-phase flow pressure drops in annular helicoidal pipe differ from that in helicoidal pipe with a circular cross-section. To the authors' knowledge, condensation heat transfer in annular helicoidal pipe has not been studied in open literature.

In this paper, the condensation heat transfer and pressure drop of refrigerant R134a in annular helicoidal pipes were investigated experimentally to further the study on the characteristics of annular helicoidal pipe flows. A series of experiments were carried out with the test section orientated at three different coil axis angles, 0° (horizontal), 45°, and 90° (vertical). The refrigerant saturation temperature and mass flow rates of refrigerant and cooling water were varied to investigate the effects of these parameters. Comparisons of condensation in equivalent smooth straight pipe and helicoidal pipe were also conducted for the performance evaluation of the annular helicoidal pipe flows.

## 2. Experimental system

A schematic representation of the experimental system for condensation heat transfer in annular helicoidal pipes is shown in Fig. 1. The system consists of two loops: a refrigerant loop and a water loop. Liquid refrigerant was pumped from a storage tank to a boiler with a positive displacement pump, which allows oil-free circulation in the refrigerant loop. A bypass was installed between the pump outlet and the storage tank to regulate the refrigerant flow to the boiler. The refrigerant was heated from liquid state to vapor with temperature-controlled electric heaters. A superheater was connected to the outlet of the boiler to heat the refrigerant to a temperature slightly higher than the saturation temperature to maintain the saturation temperature of refrigerant at the entrance of the helicoidal pipe. When the superheated vapor flowed through a flow meter, its mass flow rate was measured. After the flow rate measurement, the refrigerant vapor entered the helicoidal pipe test section, where cooling was applied and condensation heat transfer occurred. The vapor may be fully condensed, or some vapor may remain at the exit of the helicoidal pipe, depending on the cooling conditions. A helicoidal post-condenser, identical to the test section configuration, was installed downstream of the test section to

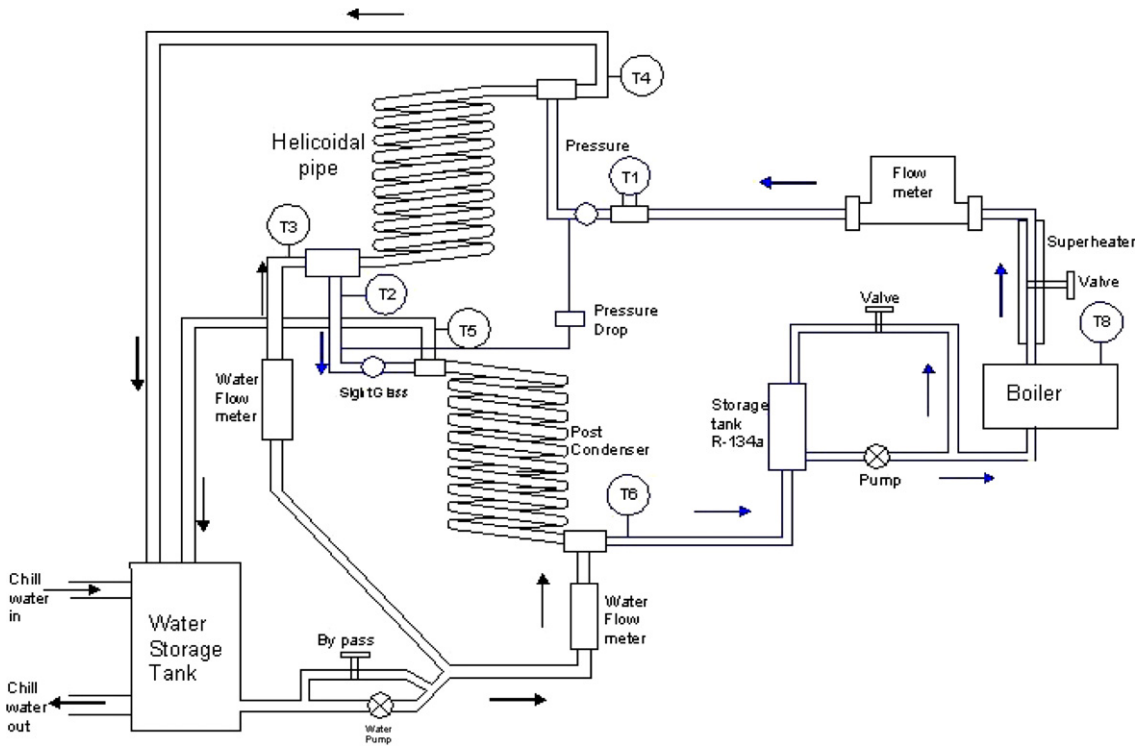


Fig. 1. Schematic diagram of the experimental facility.

cool down any remaining vapor. After the refrigerant was fully condensed to liquid state, it returned to the storage tank to complete the refrigerant loop. The cooling water was introduced from the water storage tank, where the water temperature was controlled and kept constant by a chilled water circuit. The cooling water was adjusted by a bypass and pumped into the test section and the post-condenser. The water flow rate was measured by a flow meter.

The temperature and pressure of the refrigerant and cooling water were measured at different locations, as shown in Fig. 1. All the readings were collected and stored by the data acquisition system of LabVIEW for data processing and reduction. In addition, two sight glasses were installed at the exits of the helicoidal pipe test section and post-condenser to observe the flow patterns, and the whole experimental system was thermally insulated from the surroundings by a 50 mm thick glass fiber blanket.

As shown in Fig. 2, the test section was composed of annular helicoidal pipes, where the refrigerant flowed in the annular section between the inner and outer tubes,

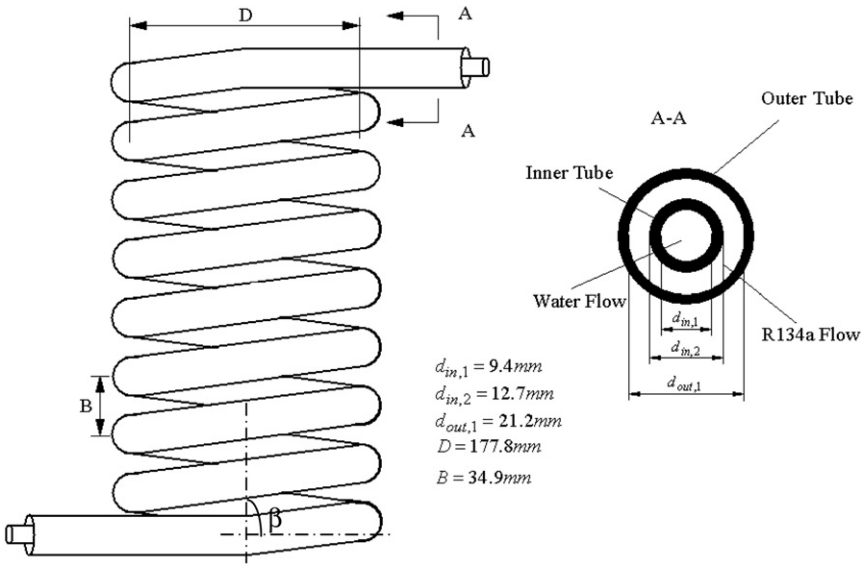


Fig. 2. Test section of the annular helicoidal pipe.

and the cooling water in the inner tube in a counter-flow direction of the refrigerant. Both the inner and outer tubes were made of copper. The tube-in-tube test section were constructed by a commercial manufacturer specialized in heat exchangers with proprietary techniques. Sampled test section was cut and inspected to ensure the cross-section of the helicoidal pipes are circular and annular. The inner diameter of the inner tube measured 9.4 mm, while that of the outer tube measured 21.2 mm. The space between the inner and outer tubes measured 8.5 mm. The coil diameter measured 177.8 mm, and the pitch of the helicoidal pipe measured 34.9 mm. The number of turns in the helicoidal pipe totaled 10. As depicted in Fig. 2, the inclination angle $\beta = 90°$ corresponds to the vertical position of the test section. The pipe length at different inclination angles is the same.

After the experimental system was thoroughly checked for leakage, the refrigerant R134a was charged into the system. All T-type thermocouples used for temperature measurements were first calibrated before installation against a precision thermometer with an accuracy of ±0.1 °C, and calibrated again in situ at three different temperatures between 20 °C and 60 °C after installation. The measurement accuracy of the thermocouples was determined as ±0.2 °C. The pressure transducers had a measurement uncertainty of ±0.25%. The flow meters measuring the mass flow rates of the refrigerant and the cooling water had an uncertainty of ±0.2%. In each test case, energy balance was calculated to verify whether the system had reached steady state. After the system had operated for more than 40 min, the energy balance deviation would be within ±10%, indicating the establishment of steady state.

Once the steady state was reached, readings of the temperature, pressure, flow rate were recorded continuously by the data acquisition system for five minutes, and the obtained values were averaged for data reduction. All thermophysical properties of the water taken from NIST [11], and that of refrigerant R134a from ASHRAE handbook [12] were correlated into a computer program to facilitate the data reduction.

## 3. Data reduction

The total heat absorbed by the cooling water can be calculated by

$$Q = \dot{V}_w \rho_w C_{pw} (T_{w,out} - T_{w,in}) \tag{1}$$

Based on Newton's cooling law, the overall heat transfer coefficient can be determined through

$$Q = U_0 A \Delta T_{LMTD} \tag{2}$$

Thus,

$$U_0 = \frac{\dot{V}_w \rho_w C_{pw} (T_{w,out} - T_{w,in})}{A \Delta T_{LMTD}} \tag{3}$$

where $\Delta T_{LMTD}$ is the logarithm mean temperature difference (LMTD) defined as

$$\Delta T_{LMTD} = \frac{(T_{f,out} - T_{w,in}) - (T_{f,in} - T_{w,out})}{\ln[(T_{f,out} - T_{w,in})/(T_{f,in} - T_{w,out})]} \tag{4}$$

From the overall heat transfer coefficient, the refrigerant side heat transfer coefficient $H_f$ can be determined by

$$H_f = \frac{1}{\frac{1}{U_0} - \frac{1}{H_w} - R} \tag{5}$$

where $R$ denotes the heat transfer resistance of the inner tube, and $H_w$ represents the cooling water heat transfer coefficient, determined by

$$H_w = \frac{Nu_w k_w}{d_{in,1}} \tag{6}$$

where $Nu_w$ stands for the Nusselt number of the cooling water. A similar method as summarized in Ref. [4] was used for the calculations of $Nu_w$.

From Eq. (5), the refrigerant Nusselt number can be calculated via $Nu_f = H_f k_f/(d_{out,1} - d_{in,2})$, where $d_{out,1} - d_{in,2}$ is the hydraulic diameter of the annular cross-section. Similarly, cooling water Reynolds number is $Re_w = \rho_w u_w d_{in,1}/\mu_w$; while refrigerant Reynolds number is $Re_f = m_f(d_{out,1} - d_{in,2})/\mu_f$, where $m_f$ is the mass flux of refrigerant per unit area.

The current formula used for pressure drop data reduction in terms of liquid and vapor phase pressure drop multipliers, $\phi_L$ and $\phi_G$, and the Lockhart–Martinelli parameter $\chi$, was found not accurate for the present condensation problem in annular helicoidal pipe. A detailed discussion of pressure drop data reduction are provided in the Section 4.2.

The uncertainty analysis for this experiment was conducted through the method recommended by Moffat [13]. Based on the measurements of different variables, the uncertainty of water Reynolds number was estimated to be less than ±1.5%. The overall heat transfer coefficient displayed an uncertainty of ±9.4%, while the water heat transfer coefficient and refrigerant heat transfer coefficient had uncertainties of ±5.4% and ±15.5%, respectively.

## 4. Results and discussion

A series of test cases were performed with the Reynolds number of the cooling water ranging from 3600 to 22000, and that of refrigerant R134a from 60 to 200. The saturation temperatures of R134a were 30 °C and 35 °C, and the cooling water temperatures were 16 °C, 20 °C and 24 °C. The test section was oriented at three different angles, 0° (horizontal), 45°, and 90° (vertical). Effects of temperature, flow rate and orientation were studied individually by varying only one parameter in each test case with all others kept constant.

### 4.1. Heat transfer characteristics

Effect of refrigerant saturation temperature on the heat transfer performance was studied by maintaining the cool-

ing water temperature fixed at $T_w = 20$ °C and the cooling water flow rate fixed at 2.2 GPM (gallons per minute). When the refrigerant saturation temperature was set as $T_s = 30$ °C and 35 °C, respectively, the orientation of the test section was adjusted to $\beta = 0°$ (horizontal), 45° and 90° (vertical) alternatively. In each combination of refrigerant saturation temperature and orientation angle, only the refrigerant mass flow rate was adjusted for data collection.

As presented in Fig. 3, the refrigerant Nusselt number $Nu_f$ increased almost linearly with the increase of refrigerant Reynolds number $Re_f$, and $Nu_f$ was larger at $T_s = 30$ °C than that at $T_s = 35$ °C. This could be resulted from the fact that at lower temperature, the refrigerant latent heat is larger, leading to an increase in heat transfer capacity. It was also observed that with respect to the three orientation angles, the difference of $Nu_f$ at $T_s = 30$ °C and 35 °C was the largest at $\beta = 0°$ and smaller at $\beta = 45°$ and 90°.

Table 1 summarized the experimental study on the effect of refrigerant saturation temperature, and gave the percentage decrease of $Nu_f$ with respect to 5 °C increase of $T_s$ from 30 °C to 35 °C. The percentage decrease of $Nu_f$ was calculated as $(Nu_{f,1} - Nu_{f,2})/Nu_{f,1} \times 100\%$, where subscripts 1 and 2 represent the change from condition 1 to condition 2. $Nu_{f,1}$ and $Nu_{f,2}$ in this case represent the values of $Nu_f$ at $T_s = 30$ °C and 35 °C, respectively. Table 1 indicated that when $\beta = 0°$, with 5 °C increase of refrigerant saturation temperature, the refrigerant Nusselt number decreased 77.53% at $Re_f = 80$, 61.3% at $Re_f = 140$ and 51.73% at $Re_f = 200$. When $\beta = 90°$, with 5 °C increase of $T_s$, the $Nu_f$ decreased 14.46% at $Re_f = 80$, 26.77% at $Re_f = 140$ and 33.67% at $Re_f = 200$. As a confirmation of the observation from Fig. 3, Table 1 revealed that the percentage decrease of $Nu_f$ was the largest at $\beta = 0°$, the smallest at $\beta = 45°$ and intermediate at $\beta = 90°$ at a given $Re_f$. It was also revealed from Table 1 that the percentage decrease of $Nu_f$ increased with $Re_f$ at $\beta = 45°$ and 90° and decreased at $\beta = 0°$. This observation indicted that when the helicoidal pipe was inclined above 45° from horizontal position, the free flow capability of refrigerant R134a in the annular section could be enhanced, resulting in a larger variation of refrigerant heat transfer rate with respect to refrigerant Reynolds number.

Table 2 gave the percentage decrease of $Nu_f$ with respect to 50% drop of refrigerant flow rate by keeping the refrigerant saturation temperature constant at $T_s = 30$ °C, cooling water temperature constant at $T_w = 20$ °C, and the flow rate of cooling water constant at 2.2 GPM. With the drop of refrigerant flow rate, the total amount of heat that could be released from the refrigerant during condensation was decreased when the other parameters were kept constant, resulting in a decrease in refrigerant heat transfer rate. Table 2 indicated that 50% drop of refrigerant flow rate caused less than 50% decrease of $Nu_f$, and the percentage decrease of $Nu_f$ was close to each other for $\beta = 45°$ and 90° and a little less for $\beta = 0°$.

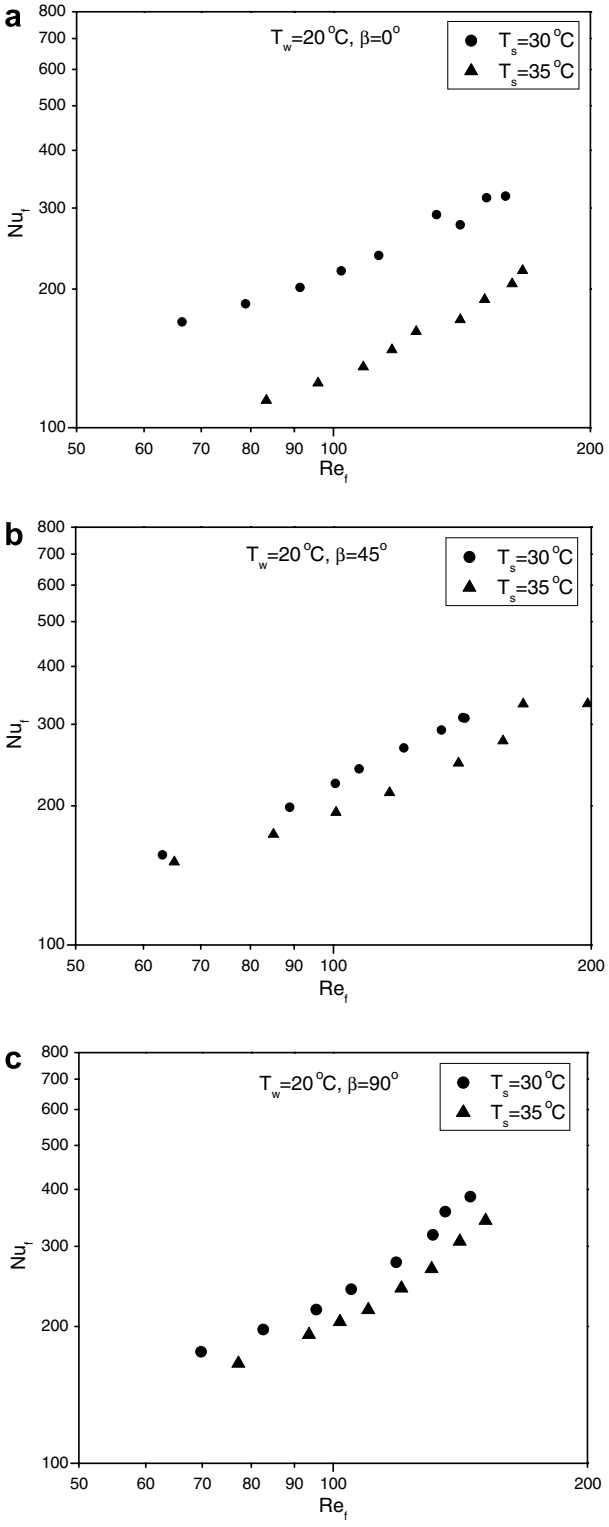


Fig. 3. Nusselt number vs. Reynolds number for refrigerant R134a at $T_w = 20$ °C. (a) $\beta = 0°$; (b) $\beta = 45°$; (c) $\beta = 90°$.

Table 3 gave the percentage decrease of $Nu_f$ when the cooling water flow rate was decreased 50%. The refrigerant saturation temperature ($T_s = 30$ °C), the cooling water temperature ($T_w = 16$ °C) and the refrigerant Reynolds number ($Re_f = 160$) were maintained constant in this case.

Table 1
Percentage decrease of $Nu_f$ with respect to 5 °C increase in $T_s$ ($T_w = 20$ °C, $\dot{V}_w = 2.2$ GPM)

| $Re_f$ | $\beta$ (%) | | |
|---|---|---|---|
| | 0° | 45° | 90° |
| 200 | 51.73 | 17.57 | 33.67 |
| 140 | 61.3 | 14.83 | 26.77 |
| 80 | 77.53 | 10.36 | 14.46 |

Table 2
Percentage decrease of $Nu_f$ with respect to 50% drop of refrigerant flow rate ($T_s = 30$ °C, $T_w = 20$ °C, $\dot{V}_w = 2.2$ GPM)

| $\beta$ (%) | | |
|---|---|---|
| 0° | 45° | 90° |
| 38.71 | 46.15 | 45.66 |

Table 3
Percentage decrease of $Nu_f$ with respect to 50% drop in cooling water flow rate ($T_s = 30$ °C, $T_w = 16$ °C, $Re_f = 160$)

| $\beta$ (%) | | |
|---|---|---|
| 0° | 45° | 90° |
| 39.43 | 45.21 | 44.45 |

As the flow rate of the cooling water was decreased, the total cooling capacity decreased, resulting in less amount of vapor to be condensed, and therefore the decrease of refrigerant heat transfer rate, as can be seen in Fig. 4, where the orientation effect was not obvious. Similar to the effect of refrigerant flow rate shown in Table 2, Table 3 also indicated that 50% drop of cooling water flow rate caused less than 50% decrease of $Nu_f$, and the percentage decrease of $Nu_f$ was close to each other for $\beta = 45°$ and 90° and a little less for $\beta = 0°$.

Table 4 presented the percentage increase of $Nu_f$ with respect to the orientation variation of the test section

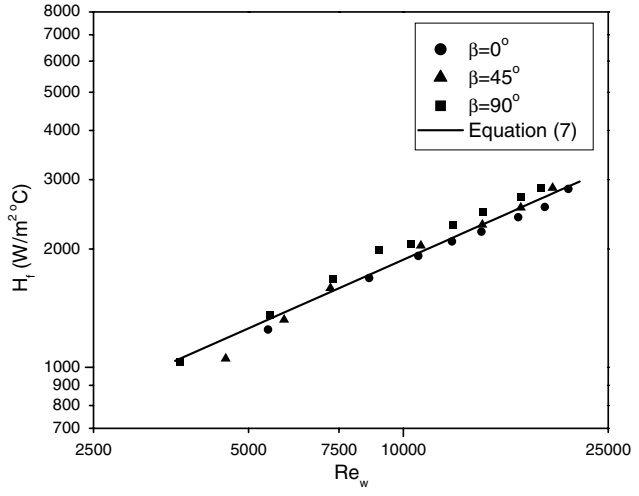


Fig. 4. Refrigerant heat transfer coefficient vs. cooling water Reynolds number.

Table 4
Percentage increase of $Nu_f$ with respect to the change in $\beta$ ($T_s = 30$ °C, $T_w = 20$ °C, $\dot{V}_w = 2.2$ GPM)

| $Re_f$ | $\beta$ (%) | | |
|---|---|---|---|
| | 0–90° | 0–45° | 45–90° |
| 200 | 15.71 | 11.17 | 5.11 |
| 140 | 13.62 | 9.89 | 4.14 |
| 80 | 10.24 | 7.84 | 2.60 |

($\beta = 0°$, 45° and 90°). At each orientation angle, the refrigerant saturation temperature ($T_s = 30$ °C), the cooling water temperature ($T_w = 20$ °C) and the flow rate of cooling water (2.2 GPM) were kept constant at $Re_f = 200$, 140 and 80. It could be observed that with the increase of orientation angle from $\beta = 0$–90°, $Nu_f$ increased 10.24% at $Re_f = 80$, 13.62% at $Re_f = 140$ and 15.71% at $Re_f = 200$. With the increase of $Re_f$, the percentage increase of $Nu_f$ also increased. From $\beta = 0$–90°, the percentage increase of $Nu_f$ from $\beta = 0$–45° accounted for more than two times of that from $\beta = 45$–90°. As explained before, the free flow capability of refrigerant R134a in the annular section could be increased much more when the helicoidal pipe was inclined from 0° to 45° compared with that at horizontal position, and increased slowly from 45° to 90°.

For the present setup, a change in cooling water flow rate or Reynolds number $Re_w$ will change the heat flux across the wall dividing the coolant and refrigerant, therefore change the heat transfer coefficient $H_f$ on the refrigerant side. This means there is a relationship between $H_f$ and $Re_w$. This relationship can be clearly observed in the experimental data presented in Fig. 4 for three values of $\beta$, which can also be correlated as

$$H_f = 8.99 Re_w^{0.58} \tag{7}$$

### 4.2. Pressure drop

The two-phase flow pressure drop multiplier in straight pipe is given by [14]

$$\phi_L^2 = 1 + \frac{20}{\chi} + \frac{1}{\chi^2} \tag{8}$$

Xin et al. [10] suggested the following correlation for two-phase flow pressure drop in vertical helicoidal pipe:

$$\phi_L^2 = 1 + \frac{10.646}{\chi} + \frac{1}{\chi^2} \tag{9}$$

As shown in Fig. 5, it could be observed that the pressure drop multipliers of the experimental data were much lower than those predicted by Lockhart–Martnelli correlation [14] or the correlation given by Xin et al. [10].

All experimental data from this study were presented in Fig. 6 in liquid phase pressure drop multiplier versus Lockhart–Martnelli parameter. Least-square fitting was used to correlate the experimental data with a correlation error of about ±6%. The developed correlation was suggested as

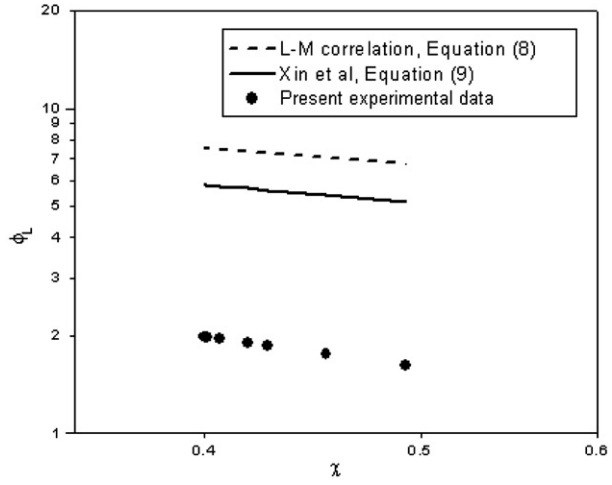


Fig. 5. Comparison of pressure drop multiplier versus Lockhart–Martnelli parameter.

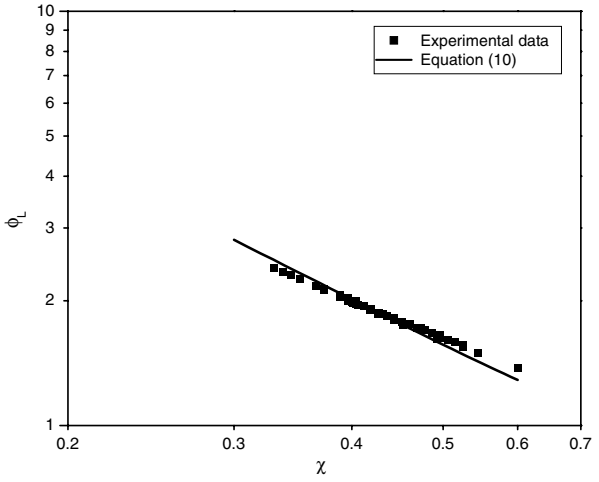


Fig. 6. $\phi_L$ vs. $\chi$ for all experimental data.

$$\phi_L^2 = 1 - \frac{1.271}{\chi} + \frac{1}{\chi^2} \tag{10}$$

Fig. 7 presented the change of liquid and vapor phase pressure drop multipliers, $\phi_L$ and $\phi_G$, with respect to Lockhart–Martinelli parameter $\chi$. The increase of $\chi$ indicated that more vapor was condensed, resulting in an increase of liquid phase pressure drop, indicated by the decrease of pressure drop multiplier $\phi_L$ as shown in Fig. 7. It was also observed that the vapor phase pressure drop decreased slightly as more vapor was condensed, and the helicoidal pipe orientation showed little effect on the pressure drop variations.

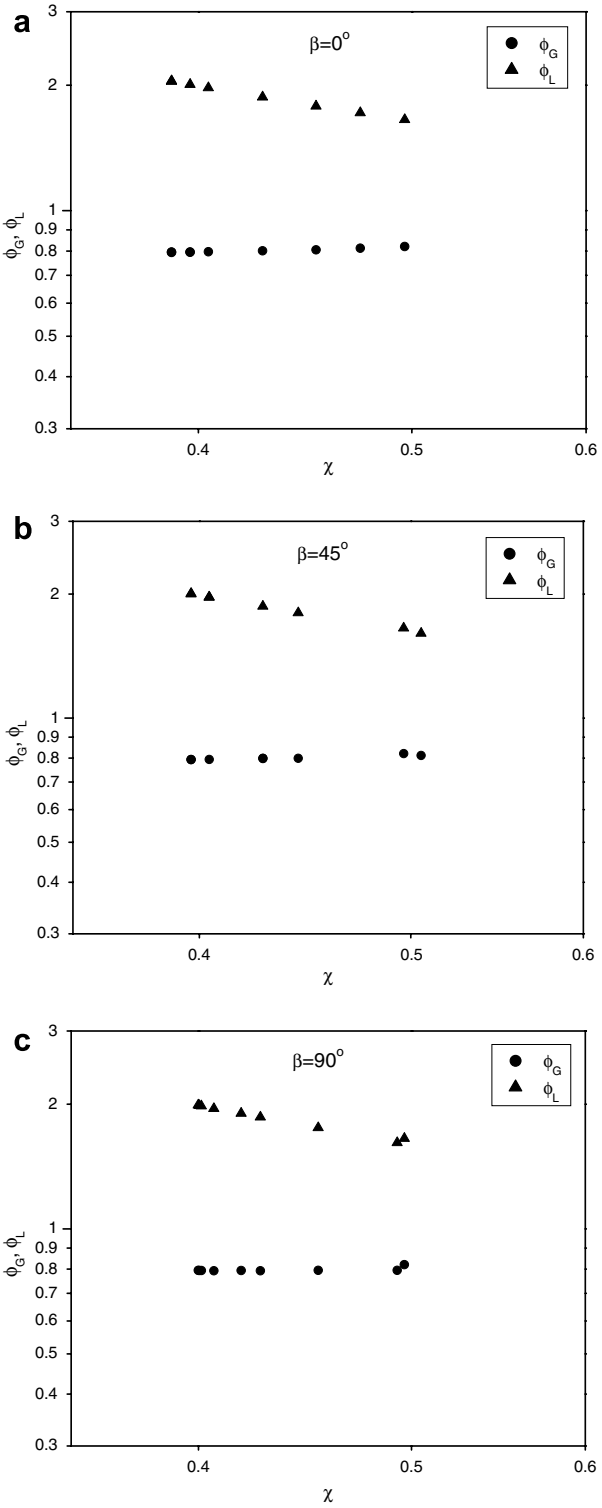


Fig. 7. Pressure drop multipliers vs. L–M parameter. (a) $\beta = 0°$; (b) $\beta = 45°$; (c) $\beta = 90°$.

### 4.3. Comparisons

Present experimental data about the condensation of refrigerant R134a in annular straight pipes were compared to the experimental data by Jung et al. [15] for R134a in a horizontal plain straight pipe with equivalent diameters and similar data range of refrigerant saturation temperature $T_s$ (40 °C) and refrigerant mass flux. The comparison was shown in Fig. 8. It can be observed that the refrigerant heat transfer rate was greatly enhanced in annular helicoidal pipe, and with the increase of refrigerant mass flow rate, the refrigerant heat transfer rate could be increased

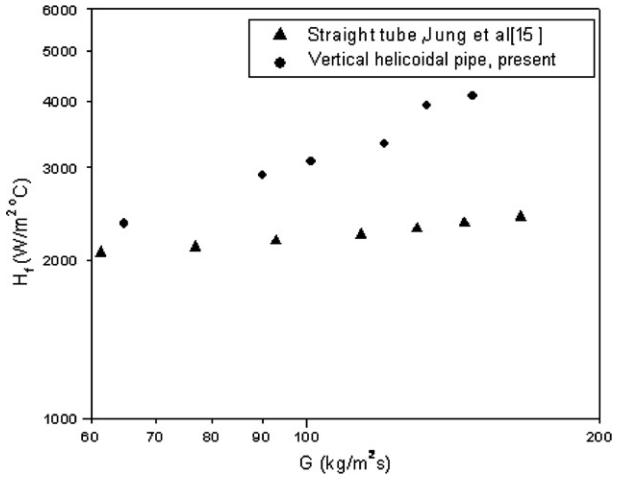


Fig. 8. Comparison of vertical helicoidal pipe's heat transfer coefficient with that of straight pipe.

up to two times of that in straight pipe at refrigerant mass flow rate above 150 kg/m$^2$s ($Re_f > 140$). The heat transfer enhancement by the annular helicoidal pipe is primarily due to the fact that the curvature of the helicoidal pipe induces secondary flow or vortex, which in turn increases the convective heat transfer rate of the flowing refrigerant.

Experimental data obtained from condensation in the traditional helicoidal pipe [4] with $\beta = 90°$ (vertical), were also compared with this study to investigate the effect of flow channel arrangement. From Fig. 9, it was observed that both heat transfer and pressure drop characteristics were quite different from previous study because of the difference in flow channel arrangement. As mentioned earlier, the change in $Re_w$ will affect $H_f$ for the present experimental system. In Fig. 9a and b, for refrigerant flowing in the traditional helicoidal pipe, the heat transfer rate of refrigerant R134a was decreasing with the increase of the Reynolds number of cooling water and the mass flow rate of refrigerant, as presented in the following correlations:

$$H_f = 12837 Re_w^{-0.32} \quad (11)$$

$$H_f = 19132 G^{-0.55} \quad (12)$$

While for refrigerant flowing in the annular section of the vertical ($\beta = 90°$) helicoidal pipe investigated in this study, the refrigerant heat transfer rate was increasing with the increase of the cooling water Reynolds number and the refrigerant mass flow rate, as presented in the following correlations:

$$H_f = 3.75 Re_w^{0.68} \quad (13)$$

$$H_f = 3.05 G^{1.31} \quad (14)$$

As shown in Fig. 9a, at $Re_w \approx 2000$, refrigerant flowing in the inner helicoidal pipe could provide two times larger $H_f$ than that in the annular section; at $Re_w \approx 4000$, refrigerant flowing in the annular section of the helicoidal pipe became better, and could have more than two times larger $H_f$ at $Re_w \approx 9000$. For the comparison in terms of the mass

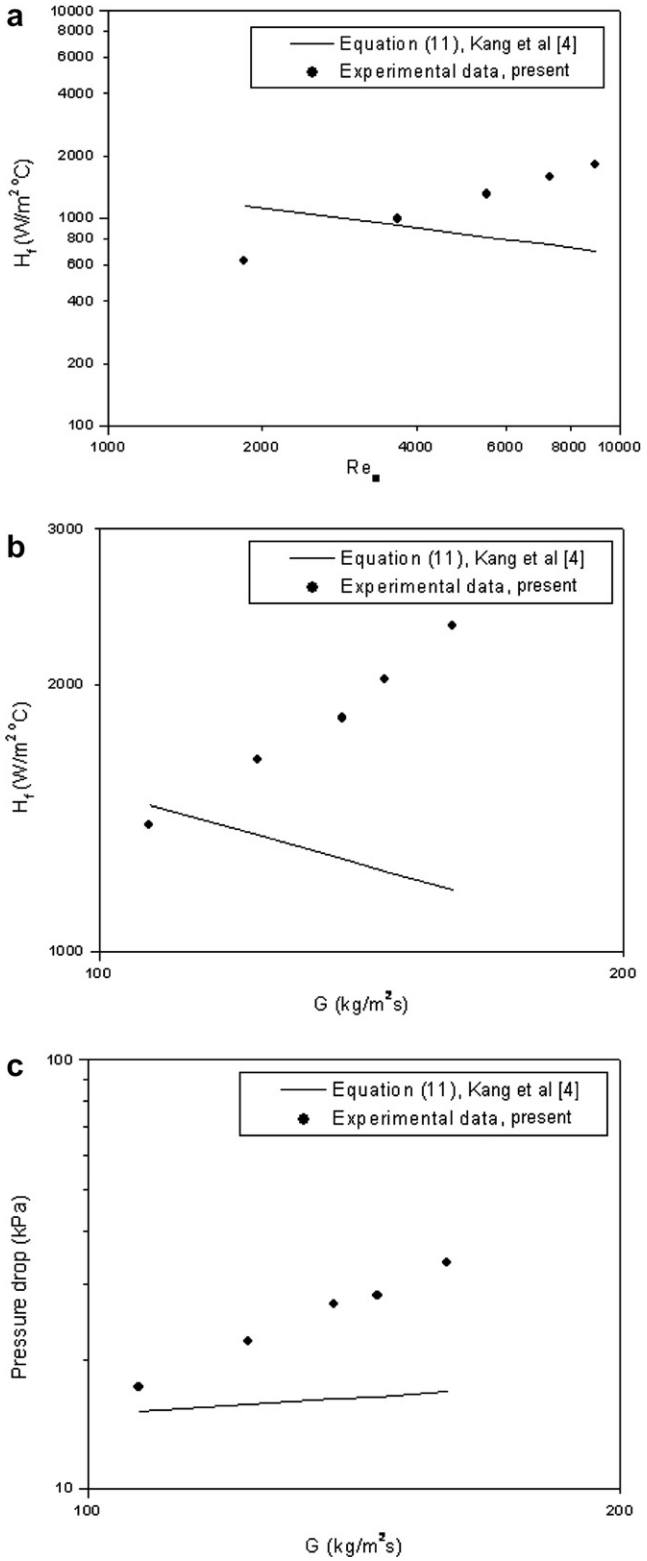


Fig. 9. Comparison with vertical helicoidal pipe having opposite flow channel arrangement. (a) $H_f$ vs. $Re_w$; (b) $H_f$ vs. $G$; (c) $\Delta P$ vs. $G$.

flow rate of refrigerant ($G$), as shown in Fig. 9b, refrigerant flowing in the annular section of the helicoidal pipe could provide about 10% less $H_f$ at $G < 110$ kg/m$^2$ s and 100% more at $G > 160$ kg/m$^2$s. This may be resulted from the fact

that the flow mechanism in the annular helicoidal pipe is different from that in the traditional helicoidal pipe, further explanation of the mechanism is under investigation.

Fig. 9c presented the comparison with respect to the pressure drop. It was observed that refrigerant flowing in the annular section of the helicoidal pipe could generate larger pressure drop than that in the inner helicoidal pipe. For refrigerant flowing in the inner helicoidal pipe [4]:

$$P_D = 4.5G^{0.26} \tag{15}$$

For that in the annular section

$$P_D = 0.0079G^{1.65} \tag{16}$$

The correlations revealed that the pressure drop could increase much larger with the increase of refrigerant mass flow rate when the refrigerant was flowing in the annular section of the helicoidal pipe than that in the inner helicoidal pipe. Beside the difference of cross-sections, the hydraulic diameter of the annular helicoidal pipe (8.5 mm) is much smaller than that of the inner helicoidal pipe (21.2 mm). Thus, at fixed flow rate, the arrangement of refrigerant flowing in the annular section of the helicoidal pipe could cause larger velocity fluctuation and turbulence variation, which could enhance the refrigerant heat transfer and in the mean time increase the pressure drop.

## 5. Conclusions

Condensation heat transfer and pressure drop characteristics of R134a in annular helicoidal pipe were experimentally investigated at three different orientations: 0° (horizontal), 45°, and 90° (vertical). Studies on the effect of individual parameter revealed that the refrigerant Nusselt number was larger at lower refrigerant saturation temperature, and would increase with the increase of mass flow rates of both refrigerant and cooling water. When the orientation increased from 0° to 90°, the percentage increase of refrigerant Nusselt number from 0° to 45° accounted for more than two times of that from 45° to 90°. When more refrigerant vapor was condensed in the annular helicoidal pipe, the liquid phase pressure drop increased while the vapor phase pressure drop decreased slightly. The orientation effect was not obvious on the pressure drop in annular helicoidal pipe flows. Compared with equivalent plain straight pipe, annular helicoidal pipe could have up to two times larger refrigerant heat transfer coefficient when the refrigerant Reynolds number was larger than 140. While compared with identical helicoidal pipe with opposite flow channel arrangement, the refrigerant heat transfer rate was larger when the refrigerant was flowing in the annular section at the water Reynolds number larger than 4000. Refrigerant flowing in the annular section would result in larger pressure drop than that in the inner helicoidal pipe.

## Acknowledgements

The authors acknowledge the financial support of DOE HBCU/MI Environmental Technology Consortium, Under Subgrant Agreement: 633254-192518, and the technical contributions from Dr. H.L. Mo and Mr. R.C. Prattipati during the course of the project.

## References

[2] M. Uddin, J. Patrick, A. Newlin, Variation of local condensation heat transfer coefficient for R-134a in helically coiled tubes, ASME Paper 94-WA/HT-4, 1994.
[3] M. Zaki, Y.Z. Liu, R.C. Xin, Z.F. Dong, M.A. Ebadian, Condensation heat transfer of R134a in helicoidal pipe, in: Proceedings of the ASME Heat Transfer Division, HTD-vol. 351, Dallas, Texas, 1997, pp. 141–148.
[4] H.J. Kang, C.X. Lin, M.A. Ebadian, Condensation heat transfer of R134a flowing inside helical pipe, Int. J. Heat Mass Transfer 43 (2000) 2553–2564.
[5] B. Yu, J.T. Han, H.J. Kang, C.X. Lin, A. Awwad, M.A. Ebadian, Condensation heat transfer of R-134a flow inside helical pipes at different orientations, Int. Commun. Heat Mass Transfer 30 (6) (2003) 745–754.
[6] S. Wongwises, M. Polsongkram, Condensation heat transfer and pressure drop of HFC-134a in a helically coiled concentric tube-intube heat exchanger, Int. J. Heat Mass Transfer 49 (2006) 4386–4398.
[7] G.T. Karahalios, Mixed-convection flow in a heated curved pipe with core, Phys. Fluids A 2 (1990) 2164–2175.
[8] S. Garimella, D.E. Richards, R.N. Christensen, Experimental investigation of heat transfer in coiled annular ducts, J. Heat Mass Transfer 37 (1998) 329–336.
[9] H.K. Choi, S.O. Park, Laminar entrance flow in curved annular ducts, Int. J. Heat Fluid Flow 13 (1992) 41–49.
[10] R.C. Xin, A. Awwad, Z.F. Dong, M.A. Ebadian, An experimental study of single-phase and two-phase flow pressure drop in annular helicoidal pipes, Int. J. Heat Fluid Flow 18 (5) (1997) 482–488.
[11] National Institute of Standards and Technology, NIST Reference Fluid Thermodynamic and Transport Properties. Boulder, Colorado, 2002.
[12] ASHRAE, Handbook of Fundamentals, American Society of Heating, Refrigerating, and Air-Conditioning Engineers, Atlanta, GA, 1997.
[13] R.J. Moffat, Describing uncertainties in experimental results, Exp. Therm. Fluid Sci. 1 (1988) 3–7.
[14] R.W. Lockhart, R.C. Martinelli, Proposed correlation of data for isothermal two-phase, two-component flow in pipes, Chem. Eng. Prog. 45 (1949) 39–48.
[15] D. Jung, Y. Cho, K. Park, Flow condensation heat transfer coefficients of R22, R134a, R407C, and R410A inside plain and microfin tubes, Int. J. Refrig. 27 (2004) 25–32.